

SANDIA REPORT

SAND2004-5636

Unlimited Release

Printed November 2004

Simulations of the Interaction of Intense Petawatt Laser Pulses with Dense Z- Pinch Plasmas

Final Report LDRD 39670

**Robert B. Campbell, Thomas A. Mehlhorn, HEDP Theory & ICF Target Design.
Dale R. Welch, Mission Research Corporation.
Joseph J. MacFarlane, Prism Computational Sciences Corporation.**

Prepared by
Sandia National Laboratories
Albuquerque, New Mexico 87185 and Livermore, California 94550

Sandia is a multiprogram laboratory operated by Sandia Corporation,
a Lockheed Martin Company, for the United States Department of Energy's
National Nuclear Security Administration under Contract DE-AC04-94AL85000.

Approved for public release; further dissemination unlimited.



Sandia National Laboratories

Issued by Sandia National Laboratories, operated for the United States Department of Energy by Sandia Corporation.

NOTICE: This report was prepared as an account of work sponsored by an agency of the United States Government. Neither the United States Government, nor any agency thereof, nor any of their employees, nor any of their contractors, subcontractors, or their employees, make any warranty, express or implied, or assume any legal liability or responsibility for the accuracy, completeness, or usefulness of any information, apparatus, product, or process disclosed, or represent that its use would not infringe privately owned rights. Reference herein to any specific commercial product, process, or service by trade name, trademark, manufacturer, or otherwise, does not necessarily constitute or imply its endorsement, recommendation, or favoring by the United States Government, any agency thereof, or any of their contractors or subcontractors. The views and opinions expressed herein do not necessarily state or reflect those of the United States Government, any agency thereof, or any of their contractors.

Printed in the United States of America. This report has been reproduced directly from the best available copy.

Available to DOE and DOE contractors from

U.S. Department of Energy
Office of Scientific and Technical Information
P.O. Box 62
Oak Ridge, TN 37831

Telephone: (865)576-8401
Facsimile: (865)576-5728
E-Mail: reports@adonis.osti.gov
Online ordering: <http://www.osti.gov/bridge>

Available to the public from

U.S. Department of Commerce
National Technical Information Service
5285 Port Royal Rd
Springfield, VA 22161

Telephone: (800)553-6847
Facsimile: (703)605-6900
E-Mail: orders@ntis.fedworld.gov
Online order: <http://www.ntis.gov/help/ordermethods.asp?loc=7-4-0#online>



SAND2004-5636
Unlimited Release
Printed November 2004

Simulations of the Interaction of Intense Petawatt Laser Pulses with Dense Z- Pinch Plasmas

Final Report LDRD 39670

**Robert B. Campbell, Thomas A. Mehlhorn,
HEDP Theory & ICF Target Design.
Sandia National Laboratories
P.O. Box 5800
Albuquerque, NM 87185-1186**

**Dale R. Welch, Mission Research Corporation.
Joseph J. MacFarlane, Prism Computational Sciences Corporation.**

Abstract

We have studied the feasibility of using the 3D fully electromagnetic implicit hybrid particle code LSP (Large Scale Plasma) to study laser plasma interactions with dense, compressed plasmas like those created with Z, and which might be created with the planned ZR. We have determined that with the proper additional physics and numerical algorithms developed during the LDRD period, LSP was transformed into a unique platform for studying such interactions. Its uniqueness stems from its ability to consider realistic compressed densities and low initial target temperatures (if required), an ability that conventional PIC codes do not possess. Through several test cases, validations, and applications to next generation machines described in this report, we have established the suitability of the code to look at fast ignition issues for ZR, as well as other high-density laser plasma interaction problems relevant to the HEDP program at Sandia (e.g. backlighting).

Acknowledgements

The authors would like to thank Roger A. Vesey for the radiation hydrodynamics calculation used as an initial condition for the Z-R simulation shown in Figure 16, left hand side. They would also like to thank Stephen A. Slutz for the $Q=1$ contour plot on which we superimposed the LSP predictions and estimates, shown in Figure 19.

Contents

1.0 Introduction and Background.....	6
2.0 Foils and beam collimation.....	7
3.0 Impact on Beam Transport from Variations in the Equation of State.....	9
4.0 3-D Beam Transport Simulations.....	10
5.0 Atomic Processes Study.....	11
6.0 Laser Plasma Interaction Simulations.....	12
7.0 LULI ion plume neutralization simulations/experiments.....	13
8.0 Fast Ignition Data Validation and Applications.....	16
9.0 Conclusions and Further Work.....	23
10.0 Publications/Reports/Presentations.....	23

List of Figures

1 Injection of relativistic electrons near $r=0, z=0$ in the positive z direction (up).....	9
2 Effect of introducing a vacuum gap surrounding a plug of aluminum.....	9
3 Three time slices of the hot electron density.....	10
4 Nine timeslices of a 3-D simulation of hot electron beam injection.....	11
5 x - y cross section (left) and y - z cross section of a relativistic electron beam propagating in full 3-D through a foil.....	12
6 Calculated mean charge state vs time for a solid density Al plasma, no hot electrons.....	12
7 Calculated mean charge state vs time for a solid density Al plasma, 10% hot electrons.....	12
8 The plasma electron density through a foil at 667 fsec.....	13
9 The electron density plotted at 667 fsec.....	14
10 Plots of kinetic electrons and protons at 4 time slices in r - Z space for the microscopic foil calculation for LULI.....	15
11 Contour plots of the laser produced electrons, the fraction of the fluid electrons now treated as kinetic (“promoted”), and the protons at 3 different times: 20, 70 and 130 psec for the macroscopic problem.....	16
12 Current traces from the simulation at $z=4$ mm, trending as in the experiments.....	17
13 Target electron density profiles (1/cc) of the pre-compressed FI GEKKO core.....	18
14 The hot electron density in the core and halo (see Figure 12) at about 4 psec.....	18
15 Contours of background electron (log) and D ion (linear) temperatures for the GEKKO case.....	19
16 Mass density from the rad-hydro simulations is on the left, the model electron density in LSP is shown on the right.....	20
17 Contours of D temperature for the case of a 2kJ PW laser heating a core with shape given by Figure 16.....	21
18 Contours analogous to Fig 17, but for a 18kJ PW laser system.....	21
19 Space of $Q=1$ contours for fast ignition cores, for $\rho d=0.6$ and a 5 psec pulse.....	22

This page intentionally left blank

1.0 Introduction and Background

The original purpose of this LDRD was first to assess the suitability of the LSP and Quicksilver code tools for the study of laser/plasma interactions with dense matter as it relates to Z and Z Beamlet/PW. Since Quicksilver did not have the ability to inject a laser pulse (although it can introduce EM energy through a waveguide arrangement), or the ability to treat the typically high-density ($1-1000 \text{ g/cm}^3$) plasmas encountered (due to its explicit algorithms), it was eliminated early in the study. However, LSP was not initially able to do what we wanted, so some development work was in order.

LSP is a 3-D implicit hybrid particle in cell code developed by Mission Research Corporation in collaboration with Sandia. For this LDRD, LSP was modified to allow a laser injection with Gaussian radial profile in both the full wave and paraxial approximation. The LMD equation of state for different materials was incorporated, as was a dynamic model for the average Z of the plasma, based on Thomas-Fermi theory coupled with the QEOS equation of state. A study was performed to determine whether in the laser plasma interaction timescales we needed to have models to follow the detailed atomic states and ionization and recombination processes. The result from that study was that for timescales slower than about 20 fsec, it was not necessary to have a microscopic multi-species model and the time asymptotic charge state for the material we studied appeared adequate.

A desirable characteristic that beams of laser-produced energetic particles should possess is that they be radially collimated. Data from foils suggest that they are not particularly well collimated, and thus may pose a problem for fast ignition scenarios that require these beams to be transported 100's of microns into high density matter. This observation motivated us to study ways in which the hot electrons could be collimated. We submitted a technical advance describing a foil with a vacuum gap that is quite effective in keeping the hot electrons radially contained. Such an idea was confirmed at ILE Osaka, and will be studied further at Sandia once the PW laser is available for experimentation. A journal article was published in Physics of Plasmas describing this method, and the reference is listed at the end of this document.

The transport laser-produced relativistic electrons through solid density foils formed the basis for the bulk of the simulation work, and was pursued in both 2-D and 3-D, with important differences noted. Later in the study, we began to include the full laser plasma interaction physics along with the transport with a good bit of success.

There were several important validation exercises performed that turned out to be of general interest in the fast ignition community, and culminated in journal articles and/or external invited talks.

The modified LSP code was used to simulate the petawatt GEKKO/PW experiments at ILE Osaka. While the original motivation was for validation, the work generated such interest that we were invited, expenses paid, to Osaka to show the results of this work. A collaboration has begun with the two prime experimentalists, Tanaka and Kodama, that has resulted in a joint paper submitted to Physical Review Letters. At this juncture, the paper is currently under review.

An extension of this work has been started, and involves the integration of the explicit laser plasma interaction and hot electron generation with the transport of the hot electrons through halo and core plasmas. This work will continue beyond the end of this LDRD.

There was some ion plume measurements performed recently on the LULI laser by Sandia personnel (M.E. Cuneo). It was important to treat behavior on the micron scale to model the laser plasma interaction, as well as on the mm to cm scale to model

the plume expanding and interacting with the cup diagnostics. We simulated these shots with LSP in a multiple-scale approach. First, the laser plasma interaction was treated with a 10 micron gold foil and LULI laser parameters. From this simulation, the plume was extracted downstream from the foil (beyond the sheath fields on the backside) and injected into a larger simulation that extends out several millimeters. The signals of electron, ion and net current from the simulation exhibit many of the characteristics of the measurements.

Major Accomplishments

- Incorporation of laser into LSP
- Development of exact implicit treatment of EM fields in LSP.
- Incorporation of LMD EOS treatment and Thomas Fermi/QEOS average charge state into LSP.
- 2-D and 3-D studies of electron beam transport through foils routinely used in experiments.
- Incorporation of K-alpha diagnostic in LSP to compare with experimental data.
- Invention of method for collimation of electron beams in filaments and plugs of dissimilar materials. A technical advance was issued for this concept and a Physics of Plasmas paper published.
- Validation of fast ignition relevant simulations with GEKKO/PW data. PRL submitted with ILE Osaka personnel.
- Simulation of ion plume neutralization data from the LULI laser.
- Simulation of Z compressed masses interacting with Z-Beamlet/PW.

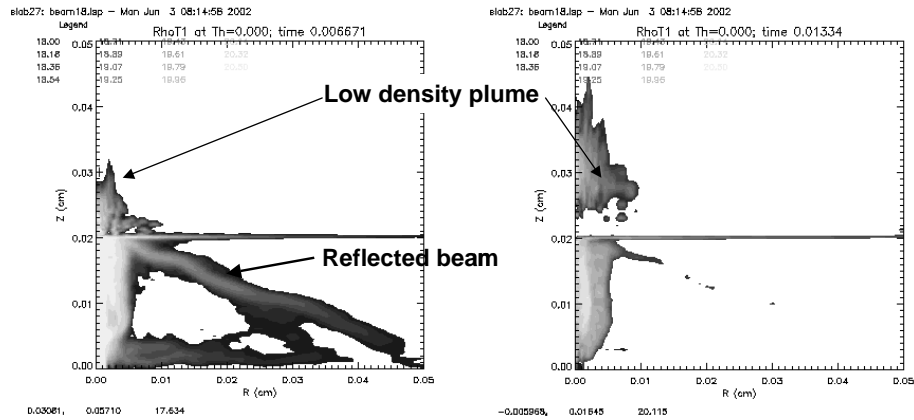
The remainder of this report will give the reader a taste of the kinds of research problems tackled during the LDRD study period. These descriptions are necessarily short and devoid of detail; the interested reader is invited to obtain the publications and talks listed at the end of the report for further edification.

2.0 Foils and beam collimation

Relativistic electron beam transport through foils of solid density was one of the first applications of LSP we tried. The implicit algorithms and fluid background electrons that LSP had made it unique it being able to solve such problems. As we looked at more and more cases, we saw quite a few similarities with experimental data, and tried to improve some of the configurations to yield more desirable performance with respect to collimating the injected beam of particles.

Electrons are injected in a 30 micron spot at $(r,z)=0$ directed in the positive z direction. The foil extends to $z=200$ microns, with a vacuum region on the backside. These simulations show the features of beam expansion, refluxing of a reflected component of the beam, and a nearly charge neutral plume of electrons and energetic ions rising from the backside of the foil. The beam size after the expansion can be up to a factor of 3-6 times the initial spot size. Experimental data also support this picture, and can be a problem when tightly collimated laser-generated beams are required to heat highly compressed matter for advanced ICF applications.

Figure 1--Injection of relativistic electrons near $r=0, z=0$ in the positive z direction (up). Illustrates the beam expansion, refluxing, and plume emission from the backside of the foil, at a time of 6 psec and 13 psec respectively.



Some large scale beam filamentation is evident

This beam expansion problem motivated us to invent a method by which the beam can be collimated and transported a distance of several hundred microns. We were granted a technical advance entitled *Method for collimation of laser generated electron beams in solid matter using radial grading of materials*. An example of the collimation idea is shown below, where an aluminum plug is surrounded by a vacuum gap. This amounts to a thin aluminum filament that the electrons are transported through. There is some unpublished data (ref R. Kodama, ILE Osaka, private communication) showing the efficacy of introducing wires in which the beam can propagate. The improved collimation in the simulation is evident from the figure.

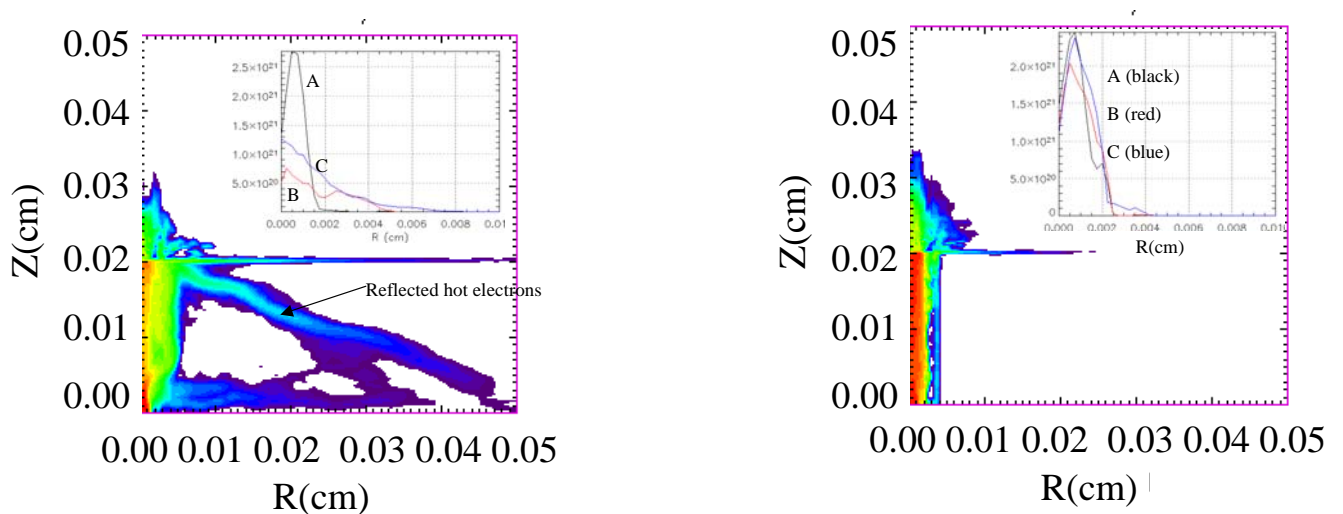


Figure 2—Effect of introducing a vacuum gap surrounding a plug of aluminum, (case with gap is on the right) on the density of hot injected electrons.

The publication section contains the reference for a Physics of Plasmas article we wrote describing in more detail the foil simulations and the collimation idea.

3.0 Impact on Beam Transport from Variations in the Equation of State

One of the questions that came up in the study of foils is how does the equation of state assumed, and the charge state of ions computed affect the propagation of the beams in foils? This is particularly relevant when starting the simulations from room temperature, solid density state. We performed simulations to test just this notion, and the results for the hot electron density are shown in the figure for a 5eV initial slab temperature. The EOS (which imply the Monte Carlo collision rate) was LMD and the charge state was a combination of the Thomas/Fermi model and QEOS. Spitzer conductivity and fixed charge state is shown on the right. Notice the beam is more filamented with the Spitzer conductivity, whereas the LMD/QEOS case the inductive fields are stronger thereby inhibiting beam propagation.

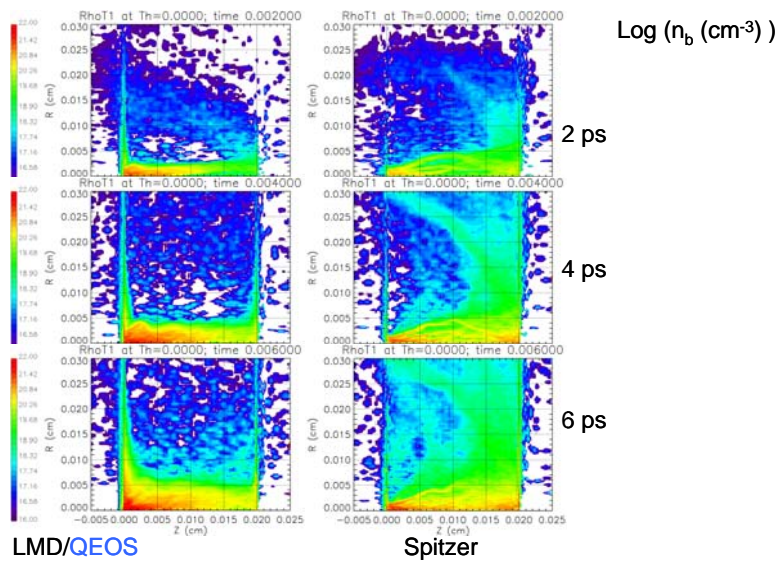


Figure 3—Three time slices of the hot electron density comparing the results using the collisionality implied LMD/QEOS equation of state with Spitzer collisionality. The beam enters from the left, near $R=0$, $Z=0$.

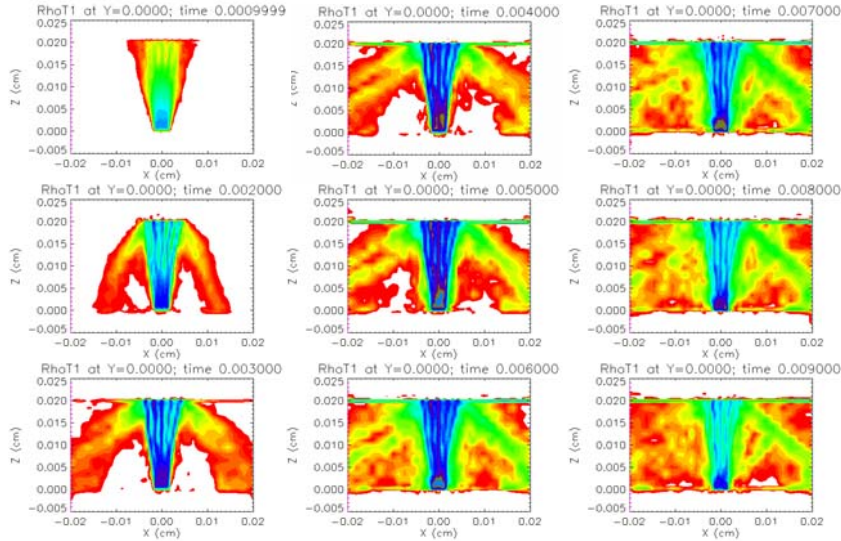
LMD/QEOS model alters beam propagation in 2D from Spitzer, in that:

- 1) LMD collision model has more conductive plasma in the 0-15 eV temperature range, beam is better pinched with no EOS
- 2) Propagation with QEOS is temperature dependent --- initial room temperature gives better beam confinement to back surface.
- 3) Peak plasma temperatures are only weakly affected by EOS

4.0 3-D Beam Transport Simulations

So far, we have shown 2d (r-z) simulations of hot electron transport in foil targets. There were several sets of 3d simulations looking at hot electron propagation in solid density foils. The first set is a direct evolution of the 2d foils already shown in the previous figures. The following figure shows the 3d analogue of the 2d simulations at timeslices from 1 to 9 psec:

Figure 4—Nine timeslices of a 3-D simulation of hot electron beam injection.



The filamentation evolves from very little at 1 psec, to a substantial amount as time approaches 9 psec. There is little $m=1$ motion, although hosing of the filaments appears to be present.

Other 3d electron beam propagation simulations were performed, mainly directed at understanding the anomalous slowing down of the beam in the presence of magnetic field filamentation. The figure below shows an example of this kind of simulation. On the left is the cross section of the foil, showing some degree of filamentation of the beam. On the right is a measure of the energy loss of the beam by tracking the relativistic $\beta\gamma$ in the z-y plane. This energy loss through the slab suggests a range of $1.6 \times 10^{-4} \text{ g/cm}^2$, which is a factor of about 1000 smaller than the classical value for this injection energy, implying that there is some kind of instability creating anomalous resistivity, the resulting electric field has the effect of slowing down the hot electrons. We shall find this same slowing down mechanism throughout the integrated fast ignition simulations to be presented later.

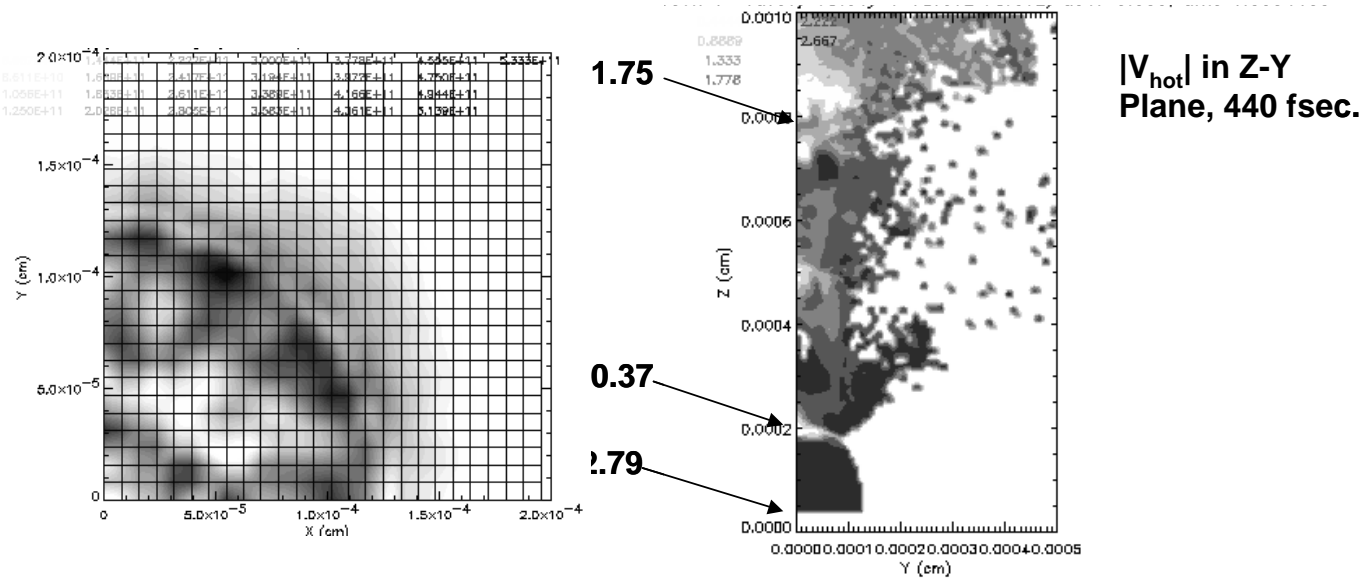


Figure 5—x-y cross section (left) and y-z cross section of a relativistic electron beam propagating in full 3-D through a foil. Filamentation (density, left) and anomalous slowing down ($\beta\gamma$, right) are shown in this figure.

5.0 Atomic Processes Study

A study was performed to determine whether in the relevant laser plasma interaction timescales we needed to have models to follow the detailed atomic states and ionization and recombination processes. The result from that study was that for timescales slower than about 20 fsec, it was not necessary to have a microscopic multi-species model and the time asymptotic charge state for the material we studied appeared adequate, even with a significant return current component at 10keV.

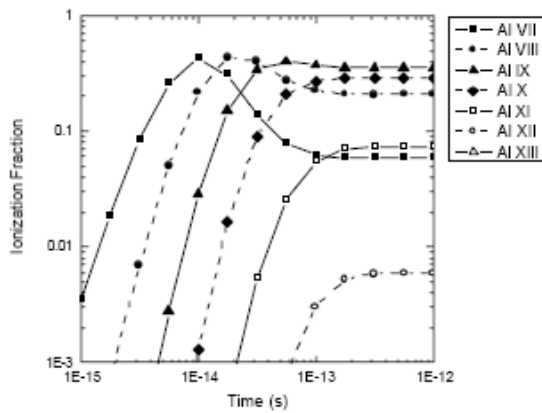


Figure 6 Calculated mean charge state vs. time for a solid density Al plasma at $T = 100$ eV and with no hot electrons.

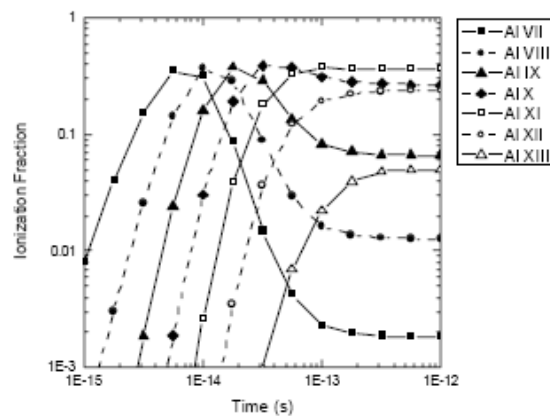


Figure 7 Same as Figure 6, but with a 10% hot electron component with $T_H = 10$ keV.

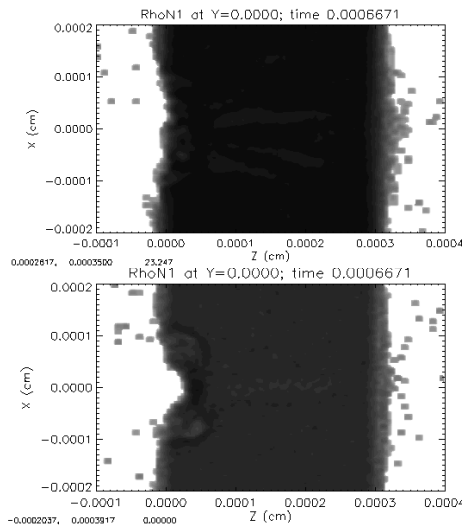
6.0 Laser Plasma Interaction Simulations

So far, we have been studying the propagation of a prescribed relativistic electron beam through the foil, where we have assumed the form for the hot electron distribution function created by the laser. It would be better if the hot electrons were self-consistently produced by laser/plasma interaction and propagated through the foil (or later to the fast ignition hot spot). One of the major accomplishments in the LSP development was to allow the code to do the laser-plasma interaction. We show several sets of simulations incorporating this new feature.

The first Laser plasma interaction (LPI) case considered was a test of the algorithms with published simulations using the code ZOHAR (Phys. Plasmas **4**, 788 (1997)). The absorption fractions agreed well, as did the partitioning of laser energy to electrons and ions.

In another LPI case we use the LSP code in a 3D mode with the explicit energy-conserving cloud-in-cell (CIC) algorithm. Using an intense laser drive, we examine the ability of the light to penetrate the plasma and the produce energetic ions with various physics activated in the code. The circularly-polarized laser pulse of 1- μm wavelength, 1- μm Gaussian profile and 10^{20} W/cm² intensity is produced with 2 dipole antennae near the left axial boundary. The simulation volume consists of a 5- μm long box with 4- μm transverse dimensions. The axial boundaries are wave-transmitting. A 3- μm thick solid-density Al⁺ foil is initialized at 10 eV beginning at $z = 0$. A comparison, with and without collisions, of the plasma electron density after 667 fs is shown in the Figure below.

Figure 8—The plasma electron density through a foil at 667 fsec. The top result shows the profile without collisions, the lower plot is the result with collisions.



The rate of penetration into the slab of the laser is roughly the same. The case without collisions exhibits a more rounded, symmetrical hole than that with collisions. The reason for this subtle difference is not well understood. A more gross difference exists when field ionization is included. Seen in Figure 9, the case with field ionization shows less hole boring and a more rapid acceleration of the back surface plasma that than the nominal case. The more rapid acceleration is obviously due to the higher charge state

plasma that exists there. The weak hole boring is likely due to the presence of a higher density plasma.

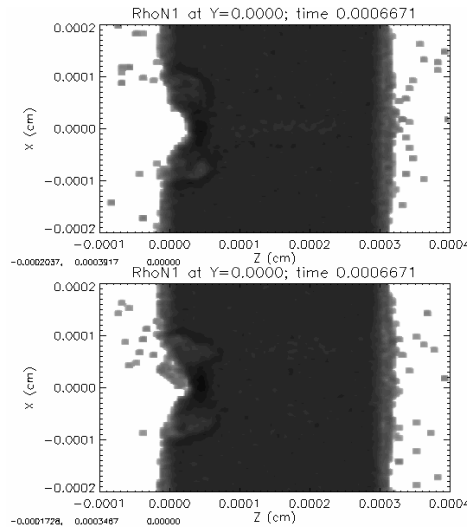


Figure 9—The electron density plotted at 667 fsec. The upper plot includes field ionization, the lower plot does not.

7.0 LULI ion plume neutralization simulations/experiments

Another application of the LPI features in LSP is the simulation of the irradiation of gold foils with the LULI laser. The goal of this work was to study the ion (hydrogen) plume leaving the back of the foil, and the degree of charge neutralization from electrons of this plume. The protons originate as a few monolayer contamination region, and are purposely laid-in in the simulation. The ability of LSP using the new models to give some of the features of the experiment is an important validation exercise. The challenges of this calculation are that the LPI is resolved, and at the same time the ion plume is followed for macroscopic distances (several cm). First performing the LPI simulation on the thin foil, and then collecting ions and electrons leaving the backside of the foil accomplish this. These captured particles are fed into a second simulation of a much larger scale, and followed on dimensions of millimeters to centimeters. Below is a set of plot of the energetic electron and proton evolution through the thin foil:

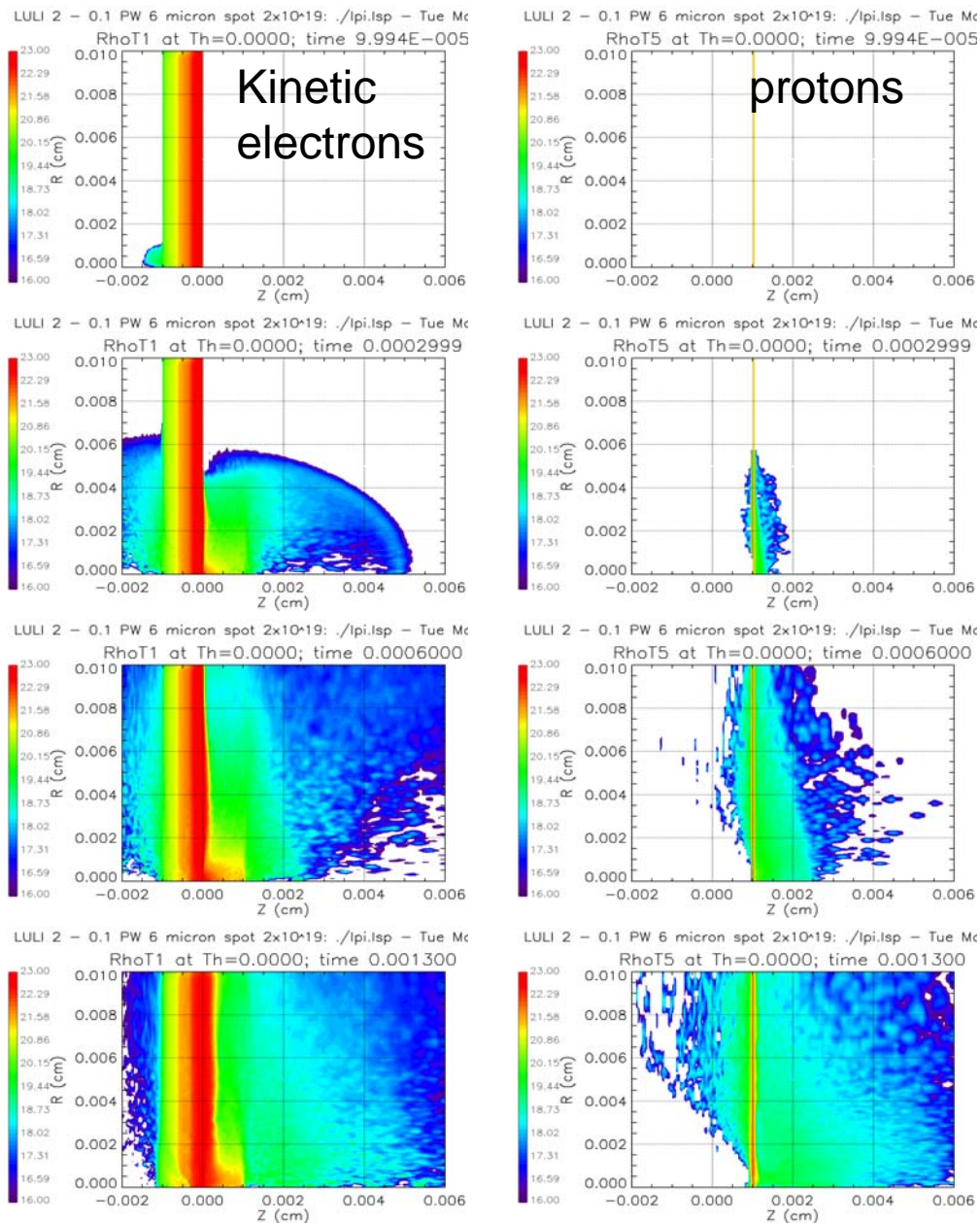


Figure 10—Plots of kinetic electrons and protons at 4 time slices in r-Z space for the microscopic foil calculation for LULI. These species are collected some distance away (85 microns) from the foil backside and launched into a “macroscopic” simulation (Fig 11)

This 10 micron foil was shown to be superior to a 50 micron foil with respect to the hot electron transport through the foil, as well as the emittance of the ion beam leaving the backside of the foil. For this case, the efficiency of converting laser light to ions is about 15%, in reasonable agreement with experimental estimates at LULI and elsewhere. The proton emittance is about 2π mm-mrad, which is quite a bit higher than what is apparently observed experimentally. The reason for this discrepancy is not well understood at present, and is an area of active study.

These results for the emitted ion and electron plumes is then inserted into a macroscopic calculation, the first of which spans a distance of about 4 mm.

Contour plots of the various density species for three time slices for this macroscopic scale simulation are shown in the figure below:

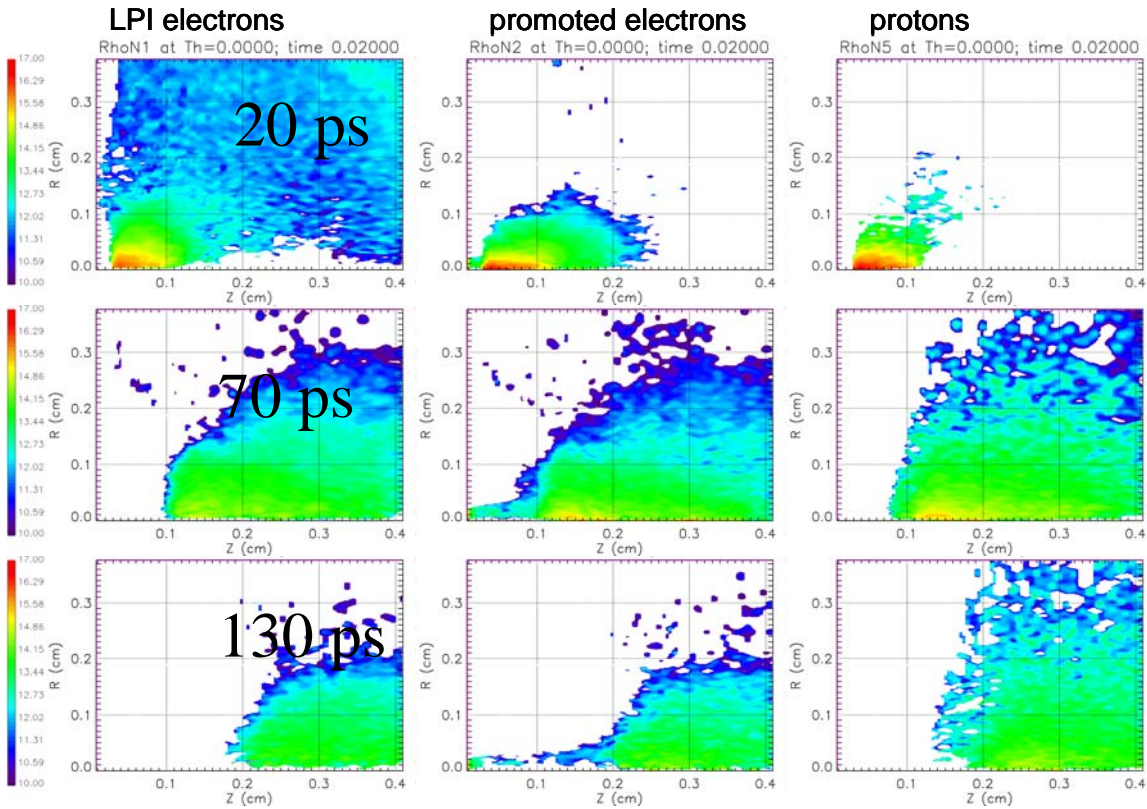


Figure 11—Contour plots of the laser produced electrons, the fraction of the fluid electrons now treated as kinetic (“promoted”), and the protons at 3 different times: 20, 70 and 130 psec for the macroscopic problem.

The promoted electrons are those that were originally fluid background electrons in the foil, and through interaction with the laser produced electrons become hot and directed enough to be treated as a second kinetic electron species. The primary experimental data are current traces from a set of Faraday cups strategically placed on either side of the line of sight of the laser. Careful shielding is necessary to avoid spurious signals from the prompt emission from the laser pulse. One of the major characteristics of the cup data is that initially the net current is negative, and over time the net current approaches zero. Below is shown traces of the currents at 4 mm as a function of time for the simulation.

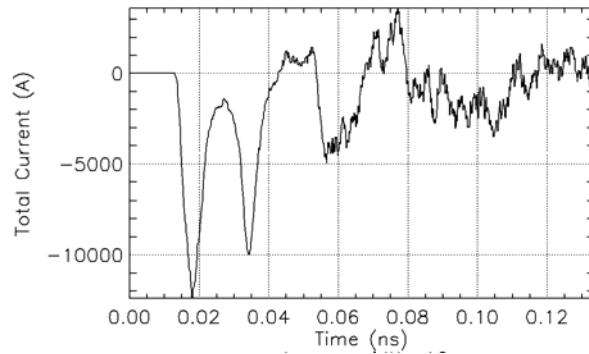


Figure 12—Current traces from the simulation at $z=4\text{mm}$, trending as in the experiments

From this figure, we see the model yields the general trend in the experimental data. More comparisons should be made with the data, but this initial quick-look is very encouraging. The conclusions of this work on LULI simulations so far are that 1) LPI and promoted or runaway electrons do sort themselves out and cool within the proton beam, 2) the trapping mechanism must be more complicated given their initial high energy, 3) as in the experiment, the electron current dominates early becoming nearly neutral late in time -- this latter point might be the most useful agreement with Faraday cup measurements; and finally, 4) as expected, a low emittance proton beam with a tail-to-head energy ramp is produced.

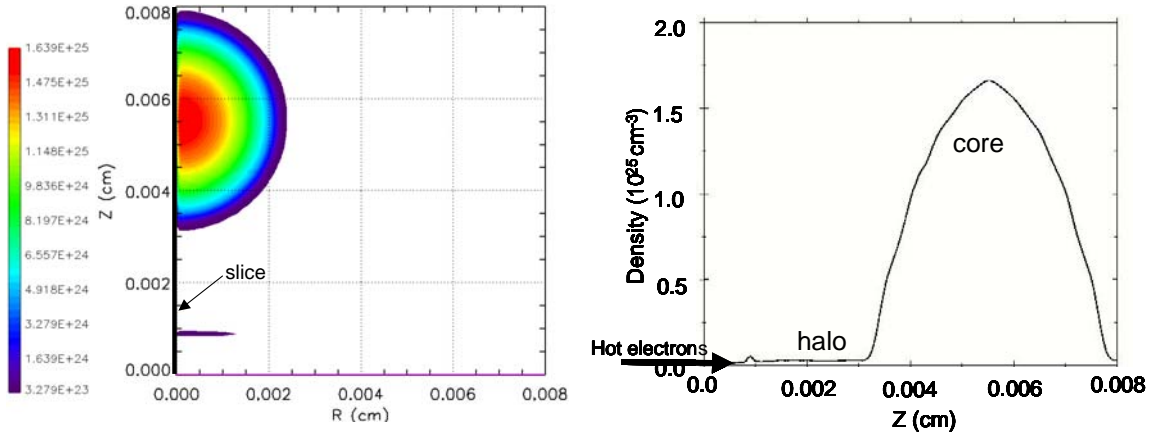
8.0 Fast Ignition Data Validation and Applications

The work so far presented in this final report is concerned with the generation and propagation of hot electrons through solid density matter. This in of itself was an important accomplishment, since standard explicit PIC codes are limited to about 0.01-0.1 solid density, even in the best case on current supercomputers. A code like LSP is uniquely suited to do these much higher densities through the use of implicit algorithms and hybrid electrons. For fast ignition, and specifically on the Z/Z-Beamlet/PW accelerator/laser system, densities much higher on the order of 100-1000 times solid must be considered. Even after the successes with the beam injection and full LPI into the solid density foils, we had some doubts as to whether the code was up to the task at very high density.

8.1 Simulations of the Osaka University Gekko/PW Experiments

As a validation exercise, we tried to simulate the recent experiments at ILE at Osaka University on the GEKKO laser coupled to their PW laser. The problem setup is one where the hot electrons are assumed to be in a relativistic Maxwellian distribution in the electron injection direction, with a specified angular spread in the transverse direction. There is a 40 micron halo surrounding the pre-compressed core (the CD core is at an average density of about 60g/cm^3) as shown in the following figure:

Figure 13—Target electron density profiles (1/cc) of the pre-compressed FI GEKKO core.



The electrons are introduced at the $(r,z)=(0,0)$ point in a full width Gaussian of 30 microns radial extent, directed in the +Z direction. To correspond to the experiment, the temperature of the hot electrons was 1.4MeV, with a 22.5 degree angular spread, and a total energy of about 100J delivered in a 600fsec full width Gaussian in time. After about 4 psec, the system has achieved a quasi-steady state, with hot electrons nearly in thermal equilibrium with the background core plasma. The logarithmic contours of the hot electron density are shown below:

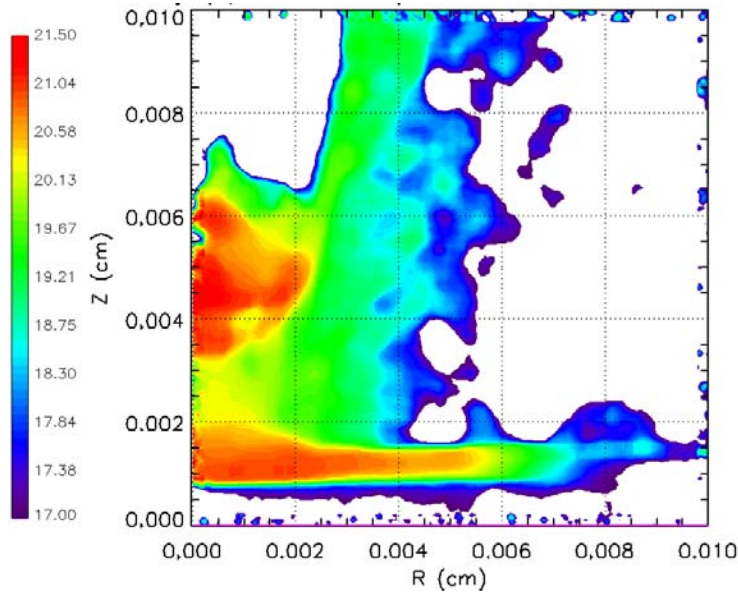


Figure 14—The hot electron density in the core and halo (see Figure 13) at about 4 psec. At this point, these electrons are in thermal equilibrium with the background core plasma.

Notice the local peaks in the density in the halo (10-20 microns) and the core (35-55 microns). The resultant energy transfer heats the background electrons in the halo to multi-kilovolt energies, and the background D,C, and electrons in the core are heated to a fusion rate weighted average of about 1 keV, in good agreement with the neutron data provided by Osaka scientists Kodama and Tanaka. Below are the color contours for the temperatures obtained from the simulation:

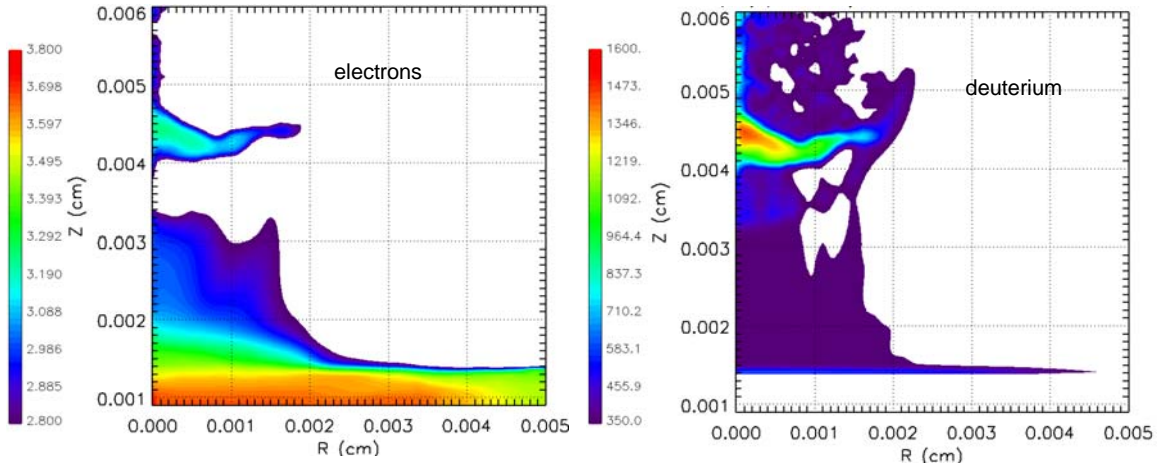


Figure 15—Contours of background electron (log) and D ion (linear) temperatures for the GEKKO case. Notice the parasitic heating of the halo region background electrons. This may be an issue for denser cores with thicker halos.

This figure shows the background temperatures of electrons and D ions in the core and the surrounding halo region. The background electrons are relatively hot in the lower density ‘halo’ region that the hot electrons must traverse. This is due to heating as a result of the establishment of the strong return current to satisfy the Alfvén current limit ($17 \beta \gamma$ kA). This parasitic halo heating reduces the energy available to heat the core and is present in all simulations we have performed, and may be of concern when scaling to higher laser intensities (larger hot electron current) and thicker halos that are likely to be present surrounding larger, denser cores.

We now compare the simulation results with the ion temperature data taken from the PW experiments. The ion temperature was measured with a neutron time-of-flight detector, showing a D temperature of 0.8 ± 0.1 keV. Figure 14b shows the linear contours of D temperature simulated by LSP for the GEKKO/PW parameters. Note that the shape of the heated region is not spherical, but instead characteristic of localized heating on the near side of the density gradient. The highest temperature in the simulation is on the order of 1.5 keV on the near side of the core, but a much larger volume at high density is at a temperature from 0.8-1.1 keV, in reasonable qualitative agreement with the data. The DD fusion reaction weighted ion temperature is the most germane for comparison with a single measurement and is about 1 keV from the simulation.

For more detailed discussion, the interested reader is referred to the publication we have recently submitted to Physical Review Letters entitled “A simulation of heating compressed fast ignition cores by petawatt laser-generated electrons”. A copy of the draft is available from the PI of this LDRD.

8.2 Sandia ZR/Z-beamlet/PW Simulations

Now that we have demonstrated that reasonable results can be obtained for an existing experiment, it would be interesting to see what the model predicts for cores more typical of those compressed in a hohlraum driven by the planned Z-R machine. The fast pulse laser used in this context is Z-Beamlet, modified for short pulse, petawatt operation. There are two operational modes chosen as representative for the Z-Beamlet/PW laser, at least in the context for fast ignition studies:

- 2kJ, 2psec Z-Beamlet/PW mid-range power/pulse single line buildout
- 18kJ, 5-20psec Z-Beamlet/PW 4 line buildout

The first mode (denoted as I) is thought to be a conservative set based on only one beamline, and delivers about 600J of relativistic electrons to the halo/core region. The second set of parameters (designated as II) is much more aggressive, requiring conversion of 4 beam lines and the use of dielectric gratings, and delivers 5.4kJ in electrons to the FI target. This latter energy level is not part of the program plan, but we thought that exploring what could be accomplished if the system were pushed near its limits might be interesting.

The initial conditions for the imploded core parameters were obtained from a rad-hydro calculation, where a hemispherical shell filled with deuterium is imploded along a gold glide plane with a Z-R driven double ended hohlraum radiation source. The resulting mass (from rad-hydro simulation) and electron density contours are shown in the figure below.

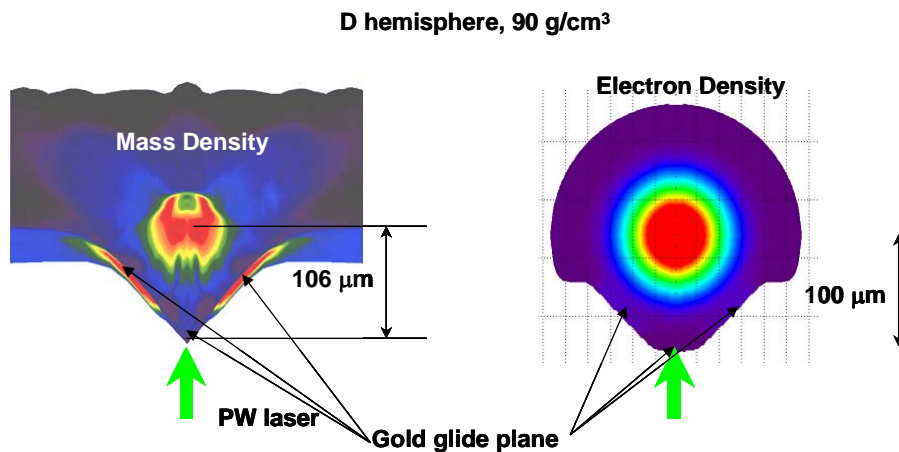


Figure 16—Mass density from the rad-hydro simulations is on the left, the model electron density in LSP is shown on the right. Important core and halo dimensions are preserved between the two representations.

The peak mass density is about 90 g/cm³, and the size of the halo and dense core are nearly the same in both the rad-hydro simulation and the density lay-in provided to LSP.

The profile of deuterium heating for the lower energy case I is shown in the next figure. This simulation assumed the same hot electron energy and angular spread as the GEKKO/PW parameters, 1.4MeV and 22.5°.

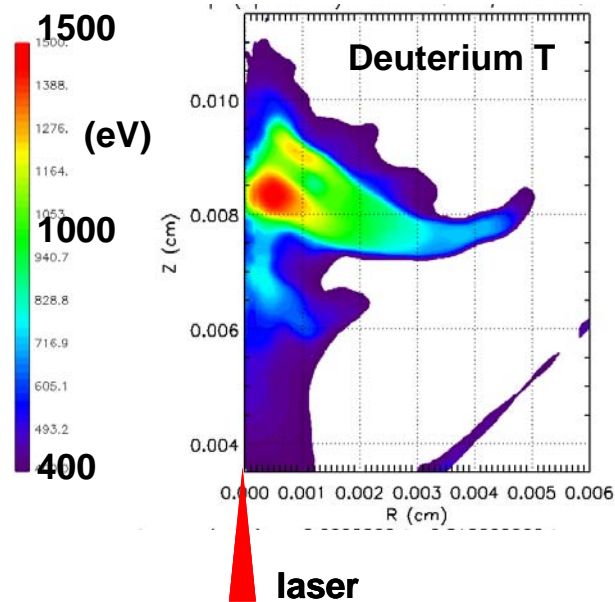
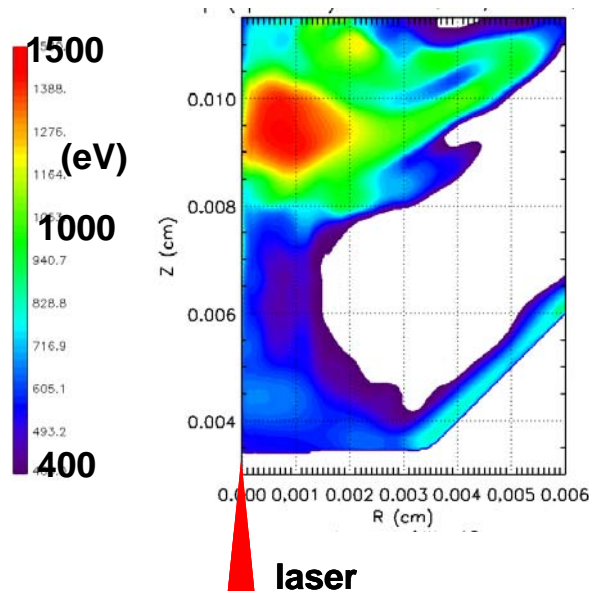


Figure 17—Contours of D temperature for the case of a 2kJ PW laser heating a core with shape given by Figure 16.

The ρr of the assembled mass is about 0.8 g/cm^2 , the heated region ρr is about 0.1 g/cm^2 , including regions above 1 keV temperature. The peak in the heating does not correspond to the peak in density, the former is on the near-side density gradient, at about 40 g/cm^3 .

The same kind of simulation, except at an 18 kJ laser level, case II is shown on the plot below. The hot electron energy was 2.75 keV , and the same angular spread as before.

Figure 18—Contours analogous to Fig 17, but for a 18 kJ PW laser system. The hot electrons penetrate deeper to high density, and the heated region becomes larger with higher delivered energy.



With the larger energy delivered to the core, the major effect is to increase the heated region, and move this region up the density gradient to about 73 g/cm^3 . The heated region ρr tripled to about 0.3 g/cm^2 , partly due to the larger heated region, and partly due to the higher heated density.

8.3 ZR Scaling to high laser energy and high density

So how do these heating results compare with the requirements for ignition or less demanding, unity fusion gain? For the 18kJ case, the fusion gain $Q = E_{\text{fus}}/E_{\text{dep}}$ fusion energy divided by energy deposited by electrons is about 0.012. This value is in reasonable agreement of analytic scaling developed by Slutz. These results were obtained at a peak mass density of approximately 100 g/cm^3 , the scaling of both ignition and $Q=1$ energy requirements scales inversely with the square of the mass density, clearly favoring higher density. Along with the higher density, the scaling laws also indicate that the size of the core must be reduced correspondingly. The need to hit a smaller target, combined with the expected thicker halo to penetrate to get the dense core may make FI core heating more challenging as the parameters approach ignition conditions. Assuming that the laser produced electrons can be sufficiently well directed to mostly be stopped in the core, and not lost around the sides of the core, the next figure shows the Q performance space of the 2kJ and 18kJ cases delivered to a capsule compressed in a dynamic hohlraum, assuming that the density was increased to 300 g/cm^3 . Rad-hydro simulations of dynamic hohlraums suggest that average densities in this range (and even higher) are indeed possible.

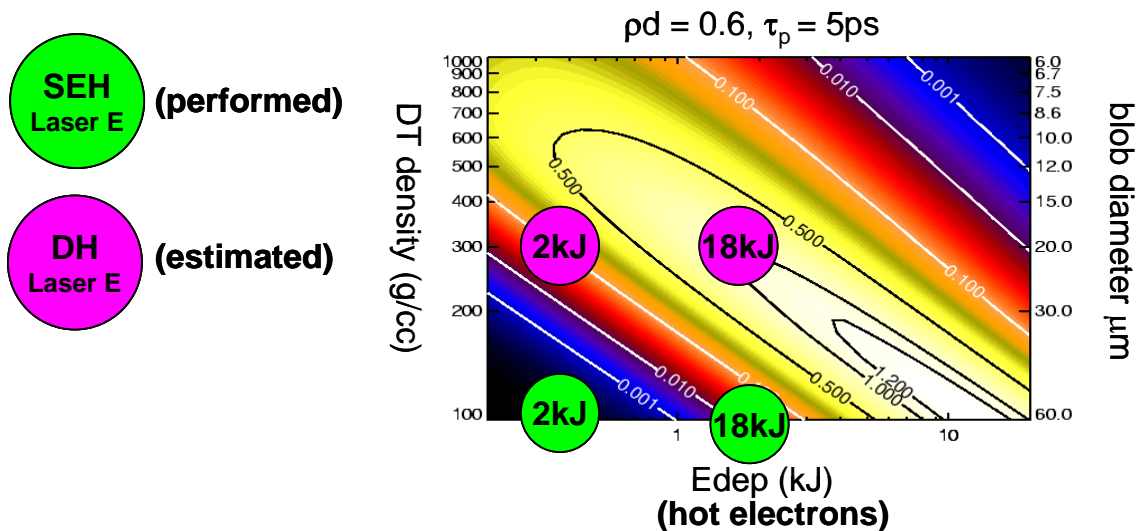


Figure 19—Space of $Q=1$ contours for fast ignition cores, for $\rho d=0.6$ and a 5 psec pulse. Superimposed are LSP simulations (green) and estimates (magenta).

In the same figure, we have also plotted the 100 g/cm^3 cases, that we actually have calculations for. Future work will study the heating physics of the higher density core, which must wait until self-consistent rad-hydro implosions are performed at the proper core compression. As can be seen from that particular figure, Q of around 0.1 would be possible at a modest 2kJ laser, and Q 's in the range of unity for the more aggressive 18kJ laser, which needs about 2 kJ deposited (5.4kJ hot electrons x 0.4 core trapping

efficiency). Whether this impressive performance is possible on Z-R with dynamic hohlraums remains to be seen, but the first step to finding out will be the simulation of the two cases at high density, and then if the results are favorable perhaps DH experiments with the new laser system operating at the 2kJ level.

9.0 Conclusions and Further Work

In the course of this LDRD, we have established that LSP is, through validation and additional code development, a viable platform to study relevant simulations of short pulse lasers interacting with dense matter. Encouraging results have been made in the areas of hot electron collimation, simulation of existing French and Japanese experiments, and exciting predictions for Z-R coupled with Z-Beamlet/PW.

There is additional work that needs to be performed to make the simulations more realistic. The main improvement needed for both the GEKKO and Z-R simulations is to include the laser plasma interaction instead of injected a prescribed distribution of hot electrons into the system. This would allow a greater degree of self-consistency in how the laser interacts with the plasma near the critical surface, and how filamentation instabilities modify the distribution in this same spatial region. Another feature that should be added is the gold cone geometry as studied experimentally in GEKKO and Omega, and proven to be advantageous over planar geometries. The gold cone tends to direct the generated hot electrons, tailor their energy spectrum, and reduce the thickness of the halo that must be traversed in order to reach the high density core. These advancements are being pursued initially as part of an Advanced Concepts for Z-pinch ICF LDRD, presently underway.

10.0 Publications/Reports/Presentations

10.1 Refereed Publications

R. B. Campbell, J. S. DeGroot, T. A. Mehlhorn, D. R. Welch and B. V. Oliver
“Collimation of PetaWatt laser-generated relativistic electron beams
propagating through solid matter” *Physics of Plasmas* 10, p4169, 2003.

R.B. Campbell, T.A. Mehlhorn, D.R. Welch, J.S. DeGroot and T.L. Marshall “Particle in cell simulations of intense relativistic electron beams propagating through solid density plasma” 11th International Conference on Emerging Nuclear Energy Systems September 29-October 4, 2002, Albuquerque, NM. p260

D. R. Welch, B. V. Oliver, and D. V. Rose, R. B. Campbell and T. A. Mehlhorn. “Hybrid Particle-in-Cell Simulation of Intense Laser-Plasma Interaction” 11th International Conference on Emerging Nuclear Energy Systems September 29-October 4, 2002, Albuquerque, NM. p269

R. B. Campbell, R.A.Vesey, S.A. Slutz, T.A. Mehlhorn, J.S. DeGroot, D.R. Welch, "Simulations of PetaWatt laser-generated electron beams in pre-compressed fast ignition hot-spot plasmas", paper WPo3.7 proceedings of the 2003 IFSA conference, September 7-12, 2003, Monterey, CA. p 461 ANS Press, #700313, 2004.

J. J. MacFarlane, I. E. Golovkin, and P. R. Woodruff, D. R. Welch and B. V. Oliver, T. A. Mehlhorn and R. B. Campbell, "Simulation of the ionization dynamics of aluminum irradiated by intense short pulse lasers". paper WPo3.3 proceedings of the 2003 IFSA conference, September 7-12, 2003, Monterey, CA. p 457 ANS Press, #700313, 2004.

D. R. Welch, B. V. Oliver, J. J. MacFarlane, R. B. Campbell and T. A. Mehlhorn "Hybrid simulation of energetic electron beam propagation in solid density aluminum". paper proceedings of the 2003 IFSA conference, September 7-12, 2003, Monterey, CA. p 398 ANS Press, #700313, 2004.

10.2. Submitted for publication

R.B. Campbell, R. Kodama, T.A.Mehlhorn, K.A. Tanaka, and D.R. Welch. "A simulation of heating compressed fast ignition cores by petawatt laser-generated electrons". Submitted to Physical Review Letters, July 2004.

10.3 Invited Talks

R.B. Campbell, T.A. Mehlhorn, and D.R. Welch. "Progress on Simulating the GEKKO/PW Experiments" Invited talk, Internal Japanese Fast Ignition and High Field Physics Workshop, Kurashiki, Japan, January 2004.

10.4 Center level external reviews

R.B. Campbell. "Fast Ignition Studies at Sandia" Trivelpiece Review of HEDP Program, May 4-6, 2004.